Characterisation of tram noise emission and contribution of the noise sources

Marie-Agnès Pallas, Joel Lelong, Roger Chatagnon

Characterisation of tram noise emission and contribution of the noise sources

M.A. Pallas[a,*], J. Lelong[a], R. Chatagnon[a]

[a] *Laboratoire Transport Environnement, INRETS, 25 avenue F. Mitterrand, case 24 69675 Bron cedex, France*

Abstract

Further to the expansion of French tram networks and related local residential complaints, a better knowledge of the situations leading to negative reactions from the local inhabitants is required. Hence a research project has been conducted to evaluate and describe noise and vibration emission of trams as well as the perception by the local residents. This paper investigates tram noise emission on common straight track sections, involving two vehicle scales. First the acoustic power and the mean vertical directivity of the total tramset is assessed using an arc of microphones. Then the localisation and the analysis of the main noise sources are performed by means of a cross-array during the tram pass-by. Two tram types representing two generations of French rolling stock, both running on two sites with distinct track characteristics, have been investigated considering the effect of speed, tram type, and track type on the noise source contributions and spectral features. Most sources are located in the lower part of the trams, mainly related to rolling noise, with a strong dependence on speed and track type. The tram type dependency, although globally of second importance, influences greatly the noise spectral distribution and behaviour. The HVAC was the only roof-mounted source which could be detected; its contribution towards building storeys becomes significant in configurations of low rolling noise. A tram noise emission model based on the various noise sources has been

*Corresponding author
Email addresses: pallas@inrets.fr (M.A. Pallas)

developed.

Key words: tram noise emission, rolling noise, traction noise, microphone array, directivity

---

1. Introduction

After trams had almost disappeared from the French urban landscape in the 50's, in those days where cars were considered as the way towards modernity, many large cities are now rediscovering this public transportation mode. For the last 20 years, new modern tram facilities have been helping cities to relieve congestion within centres, while improving their own image through clean-running public transport. Often seen as environmentally friendly, namely non-polluting and silent, trams introduce however a new component within the urban noise scene. Complaints from residents living along the lines prove that they may lead to annoyance and may be perceived as a nuisance. Within the framework of a French research programme in the area of land transportation (PREDIT), a project has been conducted to identify situations perceived as annoying, and to relate physical data concerning noise and vibration to resident perception. It included a psycho-sociological study, based on a survey of residents [1], as well as work packages dealing with vibration [2] and acoustical emission and propagation. This paper concerns the acoustical part of the project.

The tram is a complex large-sized vehicle. In standard models used for predicting noise, it is usually represented by a uniform line source. But the noise radiated by a tram actually results from the contribution of various noise sources (rolling noise, motors, auxiliary electrical equipment, HVAC[1]...) distributed along the vehicle, either spatially compact or widespread, with different physical origins (mechanic, electrical, aeroacoustic...). The development of low-floor vehicles, leading to relocated auxiliary equipment onto the roof, and simultaneously the expansion of HVAC for passenger comfort, define sources which could

[1] Heating, Ventilation and Air-Conditioning

potentially affect residents living in the storeys of buildings. Whereas some noise sources depend only on the tram equipment, others may result from the track/vehicle interaction. The type of track, as such, is a determining factor for rail and trackbed vibration, and thus for the radiated noise. Besides, the intrinsic parameters of the track, the rail and wheel roughnesses - depending on wear and maintenance - influence rolling noise. The trackbed surface also, through its absorption properties, may influence the noise propagation. Several parameters, among which running conditions such as speed, have an effect on the level and the spectral characteristics of the emitted noise, and consequently the predominance (or the screening) of some sources against others.

Except for studies dealing with specific phenomena such as squeal noise, few scientific papers are available concerning noise emission and noise sources of trams, particularly on French networks. The tram has often been considered globally, without discriminating sources. Such a detailed study was achieved in the 1980s in the Netherlands, pointing out the respective effect of several parameters (speed, type of track, type of surface...) on the global noise levels of Dutch trams [3]. Other studies (for example [4][5]) report on mean noise level improvement related to track rebuilding, where generally several parameters are simultaneously modified : rail, fastening, surfacing, commercial running speed... More recently vertical directivity was measured on an Italian tram [6] and on the Strasbourg rolling stock in France [7]. Concerning individual sources, a first investigation on the horizontal noise source distribution of the tram of Nantes was carried out in 2000, showing differences between powered and unpowered bogies, as well as frequency variations with the type of track [8]. Lately the European project SILENCE achieved a description of the noise sources of several tram types – two French, one Belgian, and one Italian – specifying the source location and spectra, as well as source ranking [9]. In that project, investigations of tram noise emission involved track types specific to each rolling stock, as well as distinct measuring protocols. The French procedure was based on several array measurements at three speeds. French and Belgian studies concluded to prevalence of rolling noise and the secondary importance – if not insignificance

– of roof mounted sources, whereas traction equipment noise was pointed out as predominant on the Italian tram.

The main objective of the present work is to specify tram noise emission, as well as the influence of several track, tram and running parameters, other parameters being equal. Noise linked to specific situations such as standstill, transient (switches, braking or moving off), or squeal in curves are outside the scope of this paper. Common conditions of running on straight track sections are considered. The first part of the work is developed in Section 2 and describes tram noise emission in free-field conditions, relying on a wide measurement campaign on the tram network of Nantes, France. Measurements include microphones in an arc for investigating noise power and vertical directivity of the whole tramset, as well as a two-dimensional microphone array for exploring the main noise sources (position, noise level, spectrum). Detailed tram noise emission is explored through several parameters - type of tram, type of track and surfacing, running speed - both for the overall tram and for the individual sources. In section 3 of this paper an empirical model of free-field tram noise emission is developed, relying on the equivalent noise sources associated to actual source areas. Model outputs are acoustic descriptors such as time signature, frequency spectrum or standard acoustic indicators. Use is made of this model for investigating the contribution of the main noise components (rolling noise, traction noise, HVAC).

2. Description of tram noise emission

Tram noise emission is approached at two distinct levels : the vehicle is firstly considered as a whole emitting object, emission information being taken through total acoustic power and vertical directivity ; then the main noise source areas are investigated.

2.1. Tram and site configurations

The measurement campaign forms the foundation of the acoustical study, and intends to state the actual noise emission for various common configurations

of French tram networks.

Two measurement sites were chosen as representative of usual closed track structures (Fig.1) : the first one is equipped with a classical track (sleepers, stiff rubber pads - stiffness 280 MN/m) and a grass surfacing, the other one has sleepers and soft pads (DPHI - stiffness 95 MN/m) and is covered by a paved surface. Thus the former offers an acoustically partly absorbent surface, whereas the latter is reflective. In each case, track structure and type of surface converge *a priori* to the same acoustical trend, either quieter or noisier. Both sites are fitted with grooved rails 35GP (mass 55 kg/m). Insulation between rail and paving is made of polyurethane foam. For each site, the rail condition can be considered as satisfactory. The roughness could only be measured at large wavelengths (0.1 m – 1.25 m), which fit the vibration frequency domain studied in parallel [2] but concern the sole lower part of acoustic frequencies : in this range, the roughness was lower than the limit curves of the reference rail of EN ISO 3095:2005 [10].

Two types of tram were measured on both measurement sites (Fig.1). The first tram (TFS, Alstom), here named *tram A*, is representative of rolling stock from the beginning of tram renewal, that is 1985-1995. It is composed of three modules, the middle one with a low floor, and has two powered and two unpowered bogies. Its total length is 39.15 m. It is equipped with DC motors, and has no HVAC. The second tram (Incentro, Bombardier), named *tram B*, is representative of the more recent tram generation (after 1995). It has a full low floor and three bogies, among which two are powered with independent wheels (one motor for each wheel, asynchronous motors). Its length is 36.14 m. The HVAC, as well as much auxiliary equipment, is roof-mounted. One tramset was available for each tram type, the same for every measurement site. Except for a slight flat on one wheel of TFS, the wheels were in good maintenance state on both trams. Both tram types have resilient wheels of 0.66 m diameter, disc braking systems and shielded bogies.

During the measurement period, the trams were running in both directions on the same track line. Records concern pass-bys at constant speeds, from 20

Figure 1: Trams and measurement sites – *left* : tram A - site with soft pads + paving – *right* : tram B - site with standard track (stiff pads) + grass

to 50 km/h, on a straight track section. Complementary measurements were also made at standstill, for studying auxiliary equipment noise.

2.2. Overall tram noise emission

2.2.1. Principle

The assessment of the noise power emitted by a tramset is based on the measurement of the noise field radiated through a virtual half-cylinder, as represented in Figure 2.

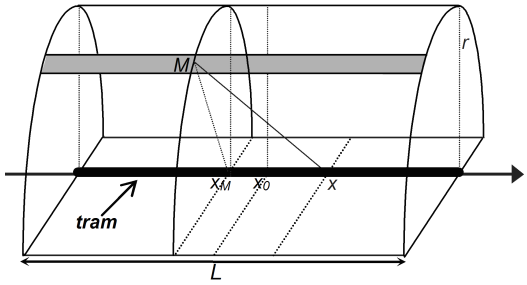

Figure 2: Evaluation of the noise power of the tram through a virtual half-cylinder

In this approach, the tram is considered as an acoustic uniform line source of length L, with a constant directivity around its axis, located on an horizontal plane. We call $W_{/m}$ the elementary power per unit length of the line source.

In the case of an absorbent ground, the apparent acoustic power $W'_{/m}$ emitted by the tram is lower than the actual tram power $W_{/m}$, and depends directly on the type of track surface.

The noise pressure is measured on the lateral surface of a half-cylinder of radius r and length L, whose axis coincides with the line source. We consider first the pressure radiated by an elementary line source section of length dx at abscissa x, received at point M of abscissa x_M located on the cylinder :

$$p^2(x_M) = \frac{\rho c}{2\pi} \frac{W'_{/m}}{r^2 + (x - x_M)^2} dx \tag{1}$$

For the whole tramset of length L, considered as a line of incoherent elementary sources whose abscissa range from $x_0 - L/2$ to $x_0 + L/2$, the squared pressure measured at point M is :

$$\begin{aligned} p_L^2(x_M) &= \frac{\rho c}{2\pi} \int_{x_0 - L/2}^{x_0 + L/2} \frac{W'_{/m}}{r^2 + (x - x_M)^2} dx \\ &= \frac{\rho c W'_{/m}}{2\pi r} \left[\arctan\left(\frac{x_M - x_0 + \frac{L}{2}}{r} \right) - \arctan\left(\frac{x_M - x_0 - \frac{L}{2}}{r} \right) \right] \end{aligned} \tag{2}$$

When integrating the squared pressure over the whole outside area S_{ext} of the half-cylinder, whose abscissa coincides with the extent of the line source:

$$\int_{S_{ext}} p_L^2(x_M) dx_M = \rho c W'_{/m} L \beta \tag{3}$$

where β is a factor depending on the length/radius ratio of the cylinder:

$$\beta = \arctan\left(\frac{L}{r} \right) - \frac{r}{2L} \ln\left(1 + \frac{L^2}{r^2} \right) \tag{4}$$

Thus the noise power radiated by the equivalent line source may be calculated by:

$$W'_{/m} L = \frac{\int_{S_{ext}} p_L^2(x_M) dx_M}{\rho c} . \frac{1}{\beta} \tag{5}$$

Application. Taking into account the order of magnitude of the tram size $L = 40$m , and if the cylinder radius is $r = 5$m, the value of β is 1.18, i.e. 0.7 dB. In such a case, the noise power $W'_{/m}$ per unit length radiated by the tram on a particular track may be approximated by the following quantity:

$$W'_{/m} \approx \frac{\int_{S_{ext}} p_L^2(x_M) dx_M}{\rho c L} \tag{6}$$

Experimental setup. At the operational level of process implementation, several microphones are arranged along an arc of a circle (outer cylinder section). Since the position of motor and auxiliary equipment on both trams presents axial symmetry, measurements are achieved only on one side of the half cylinder, assuming that acoustic symmetry is also fulfilled. Five omnidirectional microphones are regularly spaced with 12 degrees (from 6 to 54 degrees) on an arc of radius 5.1 metres centred on the tram axis. Because of the safety gauge, no microphone could be set over the upper part of the trams. Uniform vertical directivity is supposed in each angle section sampled by the individual microphones when evaluating (6). The length of the cylinder surface is then scanned *via* the pass-by of the tram from head to rear under this arc, and the acoustic power is estimated using (6) (speed effects may be ignored at tram speed).

Simultaneously, this layout allows the assessment of the actual vertical directivity of the tram, either averaged over the tram length or taken at specific tram sections.

In addition, a microphone at standard location (distance 7.5 m, height 1.2 m) was used to validate the hypothesis of uniform source line, by comparing measurements and calculation with (2) averaged on the tram pass-by duration : level differences do not exceed 0.8 dB(A) in any speed/tram/site configuration.

2.2.2. Noise power

In this section three parameters which may influence the acoustic emission of trams are considered : speed, tram type and site (i.e. track structure and surface). Figure 3 shows the global power levels per metre of both trams, regarding speed and measurement site. Variations with tram and site are summarised in table 1 at speeds of 20 and 40 km/h : for each parameter, data are referenced to the highest measured level. Similarly table 2 sums up speed variations, referenced to noise levels at 20 km/h.

The site (meaning track structure and surface) is a major parameter for noise levels, the combination of soft pads and paving being here the noisier. In this latter case, the predominance of rolling noise covers possible tram specificities

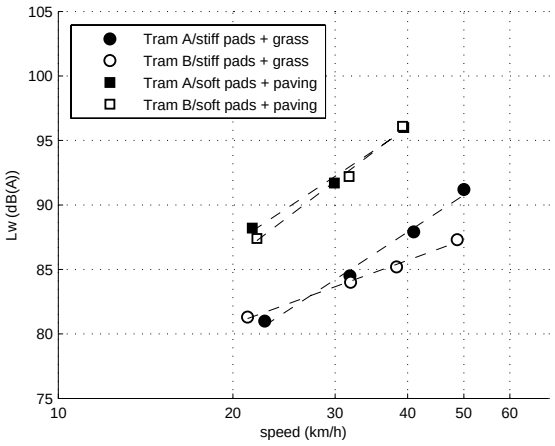

Figure 3: Global sound power level per metre length emitted by trams A and B on both sites

and differences between trams are low. However on the quieter site, the tram effect is marked and increases with speed, mainly due to frequency specificities on tram B as described below.

	20 km/h		40 km/h	
Site	soft pads + paving	stiff pads + grass	soft pads + paving	stiff pads + grass
tram A	0	-8.0	0	-8.4
tram B	0	-6.0	0	-10.6
Tram	tram A	tram B	tram A	tram B
soft pads + paving	0	-1.1	0	-0.4
stiff pads + grass	0	-1.0	0	-2.6

Table 1: Effect of site and tram types on the power levels, at 20 and 40 km/h. Levels are referenced to the highest level in each configuration.

Third octave spectral analysis of the acoustic power has been achieved in the frequency range [63 Hz – 10 kHz] (figure 4). It shows that both trams perform differently, whatever the track. Up to third octave 500 Hz, tram B levels depend

		20 km/h	40 km/h
tram A	soft pads + paving	0	+6.3
tram A	stiff pads + grass	0	+5.9
tram B	soft pads + paving	0	+7.0
tram B	stiff pads + grass	0	+2.4

Table 2: Effect of speed on the power levels. Levels are referenced to the highest level in each tram/site configuration.

very little on speed, contrary to tram A whose spectrum levels increase on the whole frequency range. On the track with stiff pads, covered with grass, power spectrum is rather spread over the frequency range, whereas it prevails in the middle frequency range for the site with soft pads. Tram B presents a constant component in third-octave 4 000 Hz which will be identified later by the noise source analysis (cf 2.3.3).

2.2.3. Vertical directivity

Vertical directivity informs on the major directions of noise emission, which is of prime importance for common prediction models, for instance for determining noise immission for residents at different storeys of buildings.

The overall tram directivity is estimated using the pass-by of the whole tramset through the 5-microphone arc setup : the mean A-weighted pressure level is calculated at each microphone, either globally or in third octaves, for each tram/site configuration. Results show that global directivity is not very marked whatever the speed, and is close to the emission of an omnidirectional source, which agrees with results from other studies [6] [7]. Despite technological differences, both tram types behave similarly. Although, slight differences may be observed between both sites (figure 5) with higher directivity close to the ground for the track with soft pads and paving.

However, directivity may be much more pronounced when considering third octaves, or when focussing on the pass-by of specific parts of the trams or source

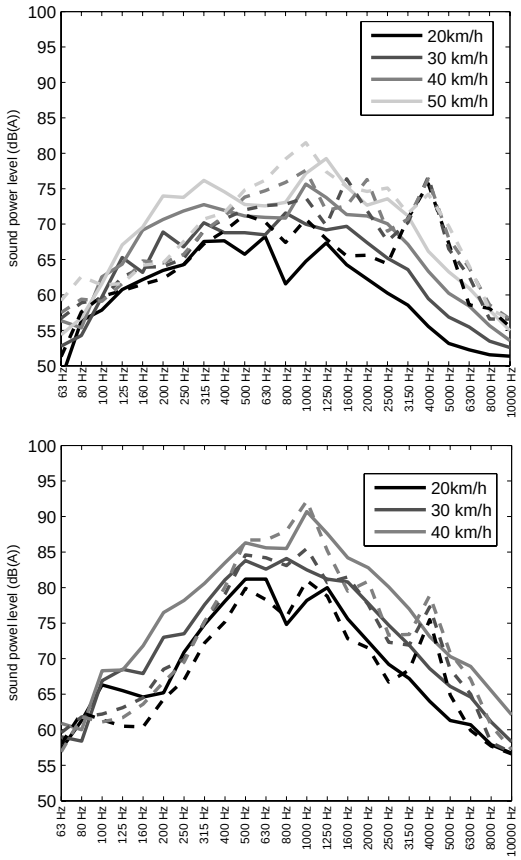

Figure 4: Power spectrum of tram A (full line) and tram B (dashed line) at 30 km/h on site with stiff pads + grass (above) and site with soft pads + paving (below)

areas. These aspects are not detailed in this paper.

2.3. Tram noise sources

2.3.1. Microphone array and processing

The second experimental approach in the acoustical part of the study considers the tram as a set of separate noise sources, characterised by their position on the tramset and their physical properties (noise level, frequency distribution). Through an appropriate measurement process, the aim is here to identify and evaluate the different noise source areas. This is achieved by implementing

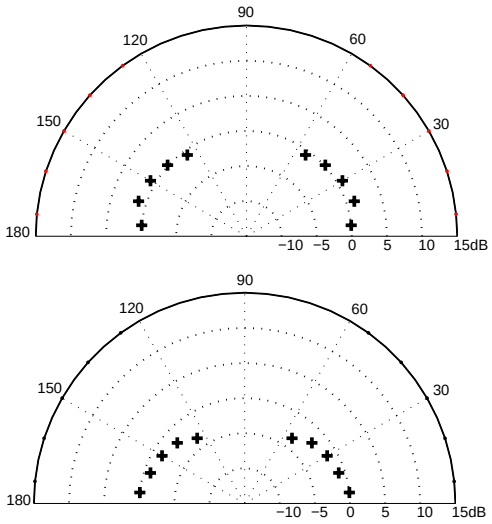

Figure 5: Mean vertical directivity of tram A at 30 km/h on site with classical track + grass (above) and site with soft pads + paving (below). A-weighted global noise levels referenced to the lowest microphone.

microphone array.

In order to locate sources in two dimensions (sideway tram emission from front to rear and from ground to roof), a two-dimensional (2D) array is needed. A correlation cross-array[2], composed of two perpendicular line arrays with equi-spaced microphones, has been selected here. This cross-array performs poorer, compared to full 2D-arrays having the same aperture with sensors distributed over the whole plane [12][13]. However, it presents several advantages : a lower number of microphones which reduces the quantity and cost of equipment necessary (sensors and multi-channel acquisition device), and the ability to select and proceed with one single linear branch when appropriate. In order to cover a wider frequency range with acceptable spatial performance, nested line arrays are implemented.

[2]Correlation cross array should not be mistaken for additive cross array, this latter offering indeed bad spatial performance [13].

In correlation cross array processing, both sensor alignments are first processed independently, involving usual line array processing [11]; then the respective line array output signals are cross-correlated [13].

If $S_{d1}(t, M)$ and $S_{d2}(t, M)$ are the output dedopplerised time signals of the two perpendicular line arrays focussed on the same point M of the vehicle, the correlation cross array signal processing achieves :

$$S_+(M) = \frac{1}{T} \int_t^{t+T} S_{d1}(t, M) S_{d2}(t, M) dt \tag{7}$$

The scan duration T at the source pass-by relies on a compromise decision between, on the one hand a better noise level estimation, and on the other hand array response distortion due to a higher scan angle and possible degradation in case of strong horizontal source directivity. $S_+(M)$ is homogeneous to the mean square value of the pressure signal coming from a point source located at the focus point and received at a reference distance r_{ref}. It can be given in dB (or dB(A)):

$$L_+(M) = 10 \log \left(|S_+(M)| / p_0^2 \right) \tag{8}$$

with $p_0 = 2.10^{-5} Pa$.

2.3.2. Array and processing characteristics

In order to provide wideband frequency analysis for each pass-by while restricting the necessary microphone number, two subarrays are nested. Each line subarray consists of 13 equispaced sensors, with respective spacing 5 cm and 15 cm, requiring thus 41 microphones in all. The frequency switch from one subarray to the other occurs between third-octaves 1250 Hz and 1600 Hz. The optimal frequency range of the processing extends from third octave 315 Hz to third octave 4 000 Hz, but is actually used down to third octave 63 Hz.

The cross array spatial resolution, as for classical delay-and-sum beamforming, depends on the ratio between the wavelength of the incident wave and the array length. Thus for a given array, lower frequency implies lower resolution. The search for uniform resolution over a wide frequency range would involve the use of specific processing [15] which is not implemented here.

Two array positions are mainly used :

- horizontal-vertical cross array in bottom position — array centre around 1 metre high — favouring the listening of the lower tram part (Figure 6),
- horizontal-vertical cross array in upper position — array centre around 3 metres high — appropriate for listening to roof-mounted sources.

The array plane is 2.3 m away from the nearer rail. Kinematics data (tram position along the track, speed) are provided by an infrared cell.

Figure 6: Nested cross array in bottom position

The focus scan area is the vertical plane including the nearer rail. The array processing involves Chebychev shading, providing -20 dB maximum sidelobe level in present line array nearfield configuration, and consequently at worst -10 dB for the cross array (Figure 7). This restricts the detection abiliy of two neighbouring horizontally or vertically aligned monopole sources to a 10 dB max. difference. Possible source directivity may affect the array pattern. The integration duration T is 250 ms in any case, therefore the steering angle range is ± 17 degrees at 20 km/h and ± 30 degrees at 40 km/h centred on the lateral direction normal to motion. Each pass-by results in the edition of 2D spatial maps of pass-by noise in global and third octave dB(A) levels. Spatial-narrowband frequency mapping (FFT) using the horizontal line array are performed as well,

in order to detect the presence of spectral lines among wider components. Figure 8 illustrates the cross array wideband spatial performance at the tram scale, for the pass-by simulation of a monopole located near the second tram wheel, whose spectrum consists of equipower tones at each third octave centre, from 63 Hz to 4 000 Hz: in that case noise sources on two successive wheels of the same bogie could be clearly separated.

The noise maps form the basic material for the identification of the main noise sources and the analysis of their behaviour as a function of several parameters: speed, tram type, track type.

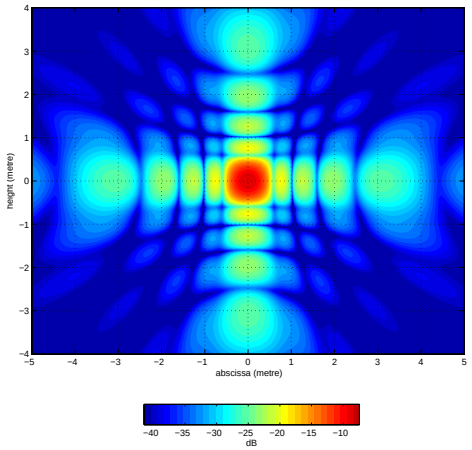

Figure 7: Cross array pattern at 1 000 Hz in actual nearfield conditions — subarray with 15 cm microphone spacing — monopole source facing the array centre

2.3.3. Identification of the main noise sources

The main noise sources which may be observed on the maps (Figure 9) are :

- the bogies and the wheels, with discrepancies between powered and unpowered bogies,
- the extended lower part of the tram

Besides, additional sources of secondary importance occur and depend on the tram type. Among these is the HVAC, which is the only source detected in the

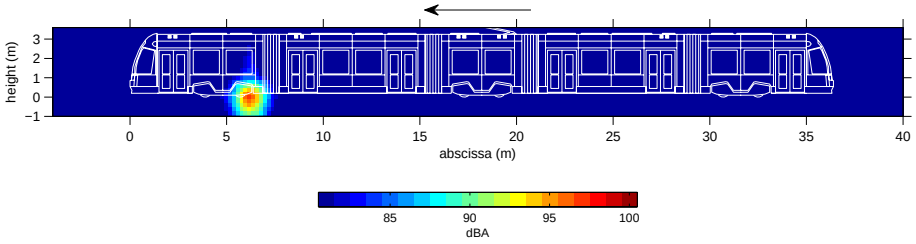

Figure 8: Cross array wideband map in dB(A) simulated for an equipower line spectrum monopole passing by at 30 km/h

upper part of the tram (tram B, since tram A has no roof equipment – except the pantograph), using the array in upper position.

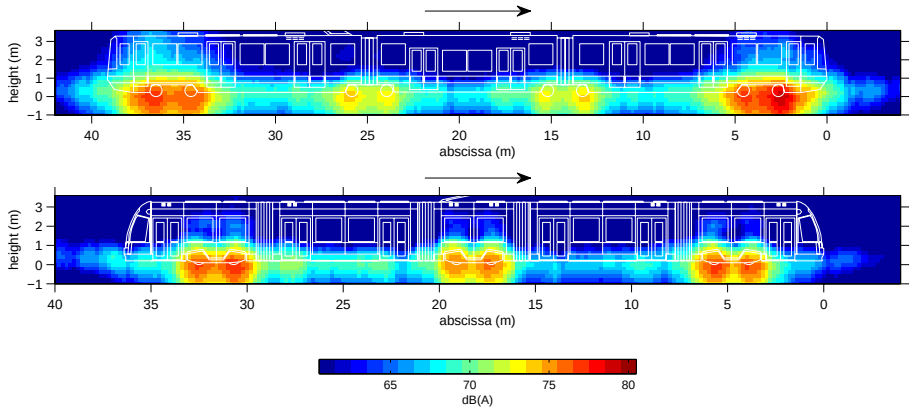

Figure 9: Global noise maps of both tram types on the site with soft pads + paving, measured with the cross array in bottom position — *above* : tram A, mean speed 30.5 km/h — *below* : tram B, mean speed 30.2 km/h — The arrow indicates the direction of movement.

The various sources differ in their spatial extent. Thus the quantitative evaluation of each source contribution will differ accordingly.

Bogie area. Predominant compact sources are the wheel areas, and more widely the bogie areas, driven by rolling noise. Bogies are shielded, thus restricting the most efficient radiating zone to the bottom part.

The array spatial performance allows the separation of successive wheels of

the same bogie over a large part of the frequency range. However the quantitative estimation of each wheel contribution may be perturbed by the presence of the wheel on the next axle, as well as other possible neighbouring sources, at least at low frequencies. It is preferable here to gather all contributions occurring within one bogie, and to consider one unique source for each bogie on the whole frequency range, called *bogie area*. It includes then the noise contribution of: both successive wheels, other parts of the bogie, the section of rail and track within the bogie area, possible neighbouring motor or devices. The noise pressure level associated to the equivalent point source is determined by detecting the maximum pressure level when the bogie passes by the vertical line array, in each third octave band. The global pressure level is calculated by energy-summation of the third octaves. No information is available concerning the wheel roughness: in order to study the mean behaviour for each bogie type, all bogies of the same kind (either powered or unpowered) are gathered within respective data sets.

Figure 10 sums up all global noise results for the various parameters: speed, bogie type, tram type, track type. The handling of pressure levels is preferred here to acoustic power levels, since the latter would imply the presumption of some source directivity whereas it is not fully available. These are A-weighted noise pressure levels at the array centre (2.3 m from the nearer rail, height 1 m). There is a higher dispersion on powered bogie levels, partly due to a large variability of tonal component levels in the spectrum.

Speed is a major parameter for the bogie area. The global pressure level rise is mainly within 7-10 dB(A) when increasing speed from 20 up to 40 km/h, according to tram, track and bogie types (Table 3). But this trend differs greatly with frequency: no effect in some third octaves, monotonic increase in others, or tone sliding. By way of illustration, Table 4 gives the slope α of the regression line, computed on the pressure level in dB(A) $L_p(v) = \alpha \log(\frac{v}{v_0}) + L_{p0}$ as a function of the tram speed v, for the powered bogies of tram B on the track with stiff pads and grass, in every third octave band; it points out the main speed dependence of the 800-2500 Hz range in this case.

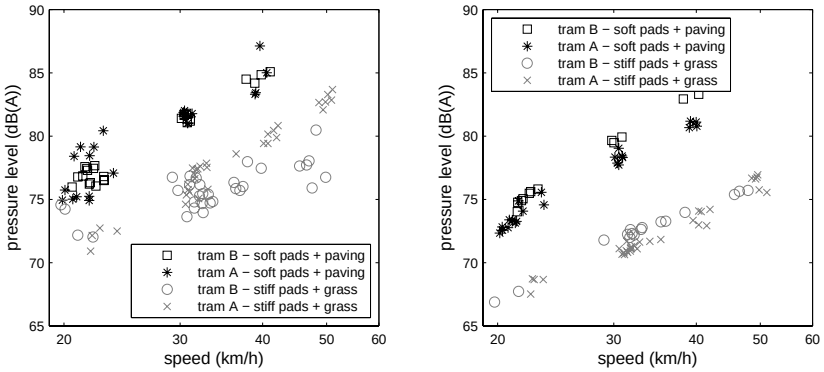

Figure 10: Global *bogie area* A-weighted noise pressure level, at the array centre — left : powered bogies — right : unpowered bogies

		tram A	tram B
stiff pads + grass	20 km/h	70.5 (*67.6*)	73.4 (*67.1*)
	40 km/h	79.7 (*73.5*)	76.7 (*74.4*)
soft pads + paving	20 km/h	75.9 (*72.5*)	75.7 (*73.5*)
	40 km/h	84.8 (*81.0*)	84.9 (*83.3*)

Table 3: Average global noise pressure level in dB(A) at the array centre from the powered (*unpowered*) bogie area, at 20 and 40 km/h

Powered bogie areas are noisier than unpowered ones, since in the former case motor contribution is also included and gives rise to the presence of tonal or narrowband components in the spectra[3]: the predominance of powered bogie areas varies over the frequency range, and depends strongly on the tram type (figure 11). For tram B for instance, discrepancies occur mainly at medium and high frequencies, including a large difference in third octave 4 000 Hz. The cross array precisely locates this 4 000 Hz powered bogie area contribution on the wheel-motors position. For tram A, the powered bogie area is noisier than

[3]However, strictly speaking, possible contribution of differences in wheel roughness cannot be totally dismissed, since relevant physical data is unavailable.

1/3 octave (Hz)	α	1/3 octave (Hz)	α	1/3 octave (Hz)	α	1/3 octave (Hz)	α
63	13.1	200	9.6	630	1.2	2000	28.6
80	8.8	250	13.0	800	33.7	2500	29.9
100	2.6	315	4.0	1000	27.6	3150	0.2
125	-6.4	400	3.8	1250	28.0	4000	2.0
160	3.9	500	3.8	1600	20.3		

Table 4: Slope of the regression line computed on the pressure level radiated by the powered bogie area of tram B on the track with stiff pads and grass

the unpowered one in most third octave bands [16].

The track is a key parameter for noise emission, and concerns both the generation of rolling noise (rail roughness, track structure) and noise absorption (surface). As mentioned before, the quality of rail surface could not be checked throughout the meaningful wavelength range, but may be considered as satisfactory. Measurements estimate the site effect to reach globally 8 dB(A) for the powered bogie and 9 dB(A) for the unpowered one, at the same speed, and exceed the contribution of sole surface absorption. Differences between both sites mainly affect frequencies greater than 200 Hz, for both bogie types.

Rail-track area. Noise maps clearly point out that a specific source area spreads along the lower part of the tram. Although it is very significant in some frequency bands, it is almost nonexistent in others. The contribution of track radiation may be reasonably presumed, as well as possible sources under the tram body with (multiple) ground-body reflections.

Track radiation results from the roughness at the wheel-rail contact patch, inducing vibrations. The vibrations transmitted to the slab are likely to radiate mainly in the low frequency range, around and beyond the lower limit of the present acoustic study frequency range [2] ; they may also contribute at higher frequencies (up to 1 kHz) whereas generally negligible [14]. Furthermore, the vibrations generated at the wheel-rail contact patches propagate in the rails ; they

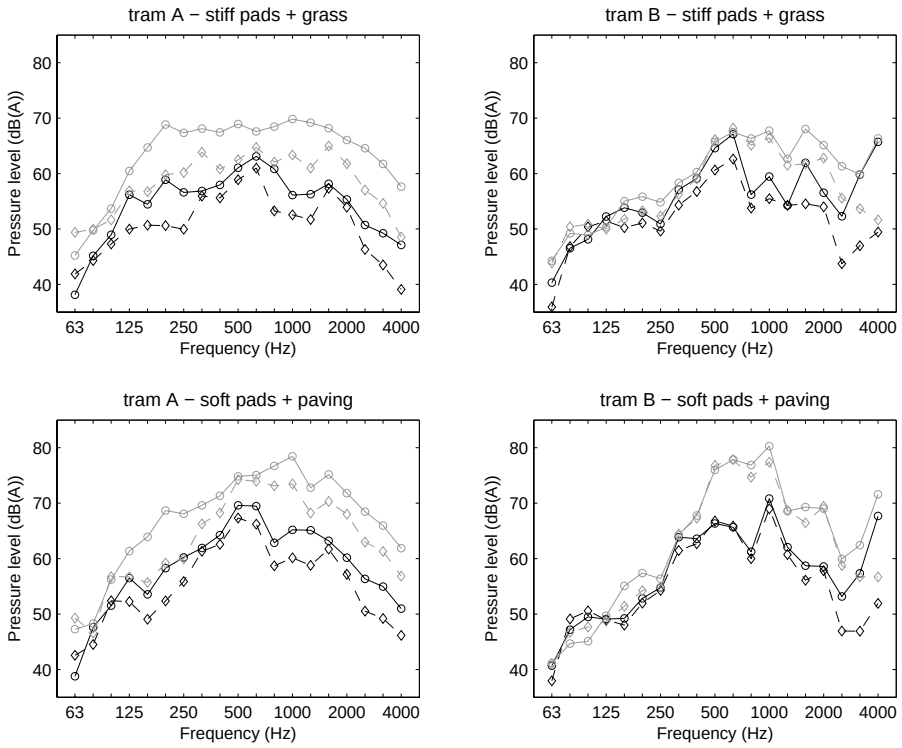

Figure 11: Third-octave spectrum from the *bogie area* at the array centre – *left* : tram A ; *right* : tram B – *above* : stiff pads + grass ; *below* : soft pads + paving ; —○— powered bogies 20 km/h ; – ◇ – unpowered bogies 20 km/h ; —○— powered bogies 40 km/h ; – ◇ – unpowered bogies 40 km/h

are characterized by their wavelength and decay rate, depending on the track structure through the mechanical parameters. In the case of closed tramway tracks, only the upper part of the rail can radiate. At a given frequency, the rail behaves like an extended coherent source, on either side of the contact area, whose extent depends on the decay rate of the vibration wave in the rail. Classical array processing states the sources to be monopoles, which does not fit the rail radiation. This has been studied in detail by T. Kitagawa in [17]: depending on the rail vibration frequency, classical array processing may under- or overestimate the actual rail noise radiation. In particular, he shows that steering the

array towards lateral direction should be preferred at high frequencies, where rail vibrations are undamped.

The processing performance in the present study does not allow the correct separation of the rail from other track source contributions, these elements here make up a whole called *rail-track source area*. The rail-track source, as seen by the array, is considered as a line source located on the ground along the rail. As a first rough approximation, it is supposed to offer slow spatial variation compared to the extent of the spatial support of the array transfer function. Even though roughly acceptable at high frequencies for the rail, this slow variation assumption becomes less reliable at low frequencies.

On the central part of each tram module distant from the bogies, no other source interferes with the rail-track source measured with the array at bottom position; in particular there is no source on the upper part. Thus the quantitative analysis has been based on the horizontal line array. A correction is included, taking account of the continuous nature of the source, involving the array spatial gain $\left|\int h(x, x_F)dx\right|$ determined in each frequency band, where $h(x, x_F)$ stands for the spatial transfer function of the array focussed at x_F (facing the array centre on the track) to a point source at abscissa x and derives from classical array processing. The process delivers the power level of an equivalent monopole with the same strength as a unit length line source section. This calculation is repeated for several positions of the centre section of each tram module in front of the array, distant from the bogies, within an horizontal interval (3.4 m for tram A and 6.2 m for tram B) over which the results are averaged with the motivation of improving the accuracy of the source level estimation using successive snapshots. Thus the variation of the source contribution in between the bogies, including rail vibration decay with distance from the wheels, is averaged at the same time, resulting in one mean level. This is denoted in the following by equivalent power level of one unit length of the rail-track area. Here it should be noticed that the separate approaches used for the evaluation of the *bogie area* and the *rail-track area* does not allow the direct comparison of their contribution ; however, this will be made possible with the

use of the model presented in section 3.

Figure 12 gives an overview of the equivalent power level per unit length, for all the running conditions tested on both sites and both trams. Once again, site effect prevails over tram type effect. But the predominance of the noise induced by one tram running on one track type does not imply its predominance on the other track. These comments on global levels may differ when considering frequency spectra.

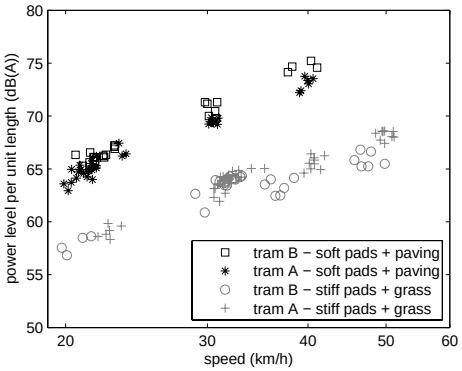

Figure 12: Rail-track area: equivalent global power level per unit length

Speed plays an important role for the rail-track source area. Table 5 gives the coefficients α and L_{W0} of the regression lines representing the average global power level $L_W = \alpha \log(v/v_0) + L_{W0}$ with $v_0 = 40$ km/h, for the various track/tram configurations, and specifies their speed validity domains. The global level increase is 6-10 dB(A) according to the tram/site configuration from 20 to 40 km/h. However, this behaviour differs from one third octave band to the other (figure 13). The speed reinforces the spectrum at middle and higher frequencies (500 to 2500 Hz) for tram B. On the other hand for tram A, speed increase affects the whole spectrum, which does not change the noise frequency distribution much [16]. These trends are similar to those observed for the bogie area, which is probably due to the decisive contribution of rolling noise in both cases.

	tram A		tram B		
	α	L_{W0} dB(A)	α	L_{W0} dB(A)	validity km/h
stiff pads + grass	24.8	82.0	20.4	81.0	[20 - 50]
soft pads + paving	30.1	89.2	32.7	90.8	[20 - 40]

Table 5: Coefficients of the regression line $L_W = \alpha \log(v/v_0) + L_{W0}$ computed on the global power level per unit track length in dB(A) associated with the rail/track area ; $v_0 = 40$ km/h

The type of track has a major influence on the rail-track source: depending on tram and speed, the track with soft pads and paving may globally be up to 10 dB(A) noisier than the stiff one. Differences occur mainly at middle and high frequencies (400-4000 Hz). However, as the rail roughness has only been partially documented, its part in these differences cannot be specified.

HVAC. HVAC contribution concerns tram B only. During the pass-by measurement campaigns on the various sites, the air-conditioner was off. However, measurements with the array at upper position show the existence of a weak source, linked to the basic ventilation device. The HVAC noise emission has been studied with a supplementary campaign, involving the five directivity microphones facing successively the bogies and the middle parts of the modules of the tram at a standstill, with HVAC either off (but with basic ventilation) or at full capacity. In this latter case, the maximum HVAC contribution may then be estimated.

Global noise pressure levels in dB(A), without and with operating HVAC, are represented in Figure 14. Rectangles stand for the microphones, their centre locations agree with the respective sensor positions. The strongest levels are met on the highest microphone when facing the HVAC location (roof at the middle of the modules), the global increase with working HVAC being around 9 dB(A). However, the increase remains noticeable along the tram, even away from the HVAC location. Moreover its contribution is not restricted to the roof area, but affects also the lowest microphones, thus showing wide horizontal and

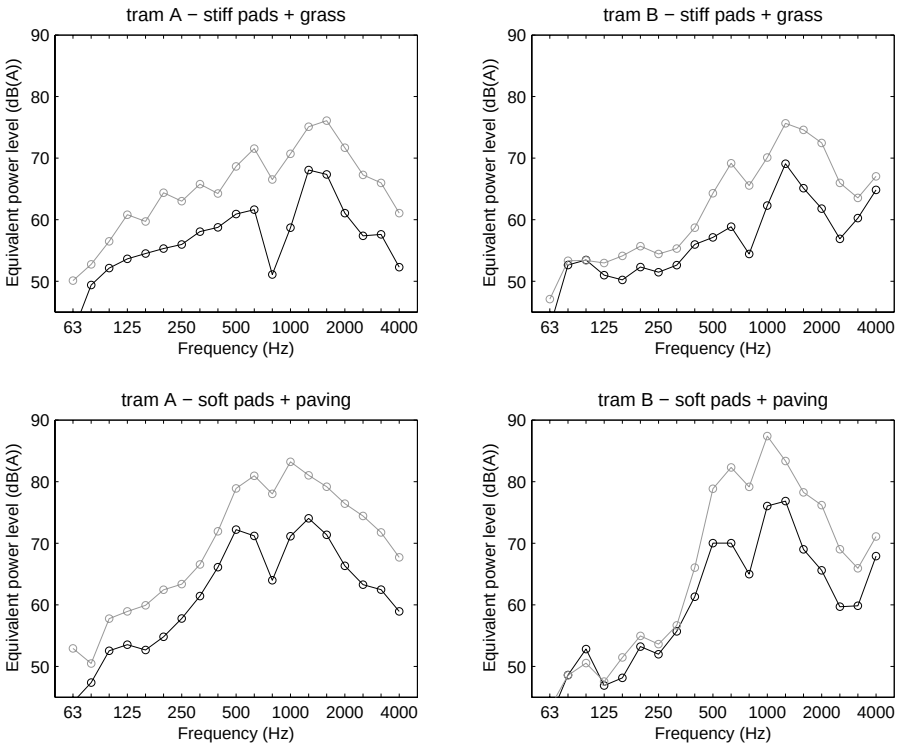

Figure 13: Rail-track area: third-octave spectrum of the equivalent power level per track unit length – *left* : tram A ; *right* : tram B – *above* : stiff pads + grass ; *below* : soft pads + paving ; —o— 20 km/h ; —o— 40 km/h

vertical directivity. Spectral analysis reveals the occurrence of one strong tonal component (290 Hz), as well as two weaker first harmonics, when the HVAC is working.

The relative part of the HVAC among the other sources will be detailed in the next section.

3. From measurements to free-field noise emission modelling

During the experiment a wide set of noise data was collected, describing the trams and their noise sources for two site types. Regression curves, where speed is the basic parameter, have been calculated. Thus for each main source,

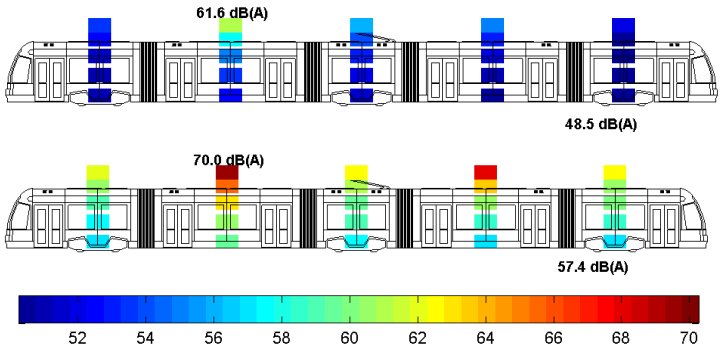

Figure 14: Global dB(A) noise pressure levels measured at standstill with HVAC off (top) and on (bottom)

several average free-field noise emission characteristics are available per {tram, site} pair:

- A-weighted noise power level $L_W(v;f)|_{tram,site}$, as a function of speed v, for each third-octave of centre frequency f — derived from the array measurement ; for HVAC : A-weighted noise power level $L_W(f)|_{tram,site}$ — derived from the directivity measurement device,
- vertical directivity $D(v,\theta_v;f)|_{tram,site}$, where in addition θ_v stands for the vertical emission angle — derived from the vertical microphone arc device. For determining the vertical directivity of the bogie area, it was stated that this was the only major noise source when facing the vertical directivity measurement device. For the rail/track area, the extended source was assumed to be the only major contribution (HVAC off) in the middle of the coaches. As for the HVAC vertical directivity it came from investigations with the tram at a standstill.

These constitute the core of the tram pass-by free-field emission model.

3.1. Description of virtual trams

A tram is seen as a set of independent sources, each of them being described by its location and extent on the tram, its third octave noise emission spec-

trum, its horizontal and vertical directivities. Virtual trams handled within the scope of this paper comply with reality, i.e structure and size, and source characteristics. Parameters are tram and track types. Four kinds of sources are introduced, linked with the main source areas detected in the previous section: powered bogies, unpowered bogies, extended track/rail area, HVAC (Figure 15).

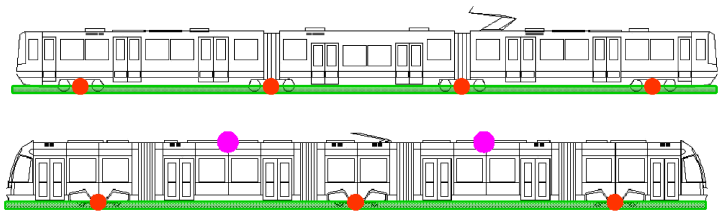

Figure 15: Tram model with sources for tram A (top) and B (bottom) – ● : point sources for powered and unpowered bogies – — : line rail/track source – ● : point sources for HVAC

The noise emission of each bogie is modelled through one point source located on the nearer rail at the abscissa of the bogie centre between the axles. The frequency spectrum and the vertical directivity are given by the previous empirical emission laws in third octaves, distinguishing between powered and unpowered ones. The horizontal directivity is arbitrarily selected as an angle cosine function, according to data available in the literature (for example [18]).

The rail/track noise contribution is introduced by a uniform line source on the nearer rail extending from tram head to rear. It is modelled by a line of identical and equidistant incoherent point sources. Each elementary source is assigned a uniform horizontal directivity. Third octave spectrum and vertical directivity result from the empirical emission laws. It may be noted that no decay rate was used on either side of the wheel-rail contact patch despite the probable contribution of rail radiation. Strictly speaking, track noise is counted twice around bogies, since it is also included within the bogie area where its part is higher due to the decay rate. Therefore, this duplication results probably in insignificant bias.

Each HVAC unit is modelled by a point source located on the longitudinal

axis at equal distance from the tram module ends. Within the scope of this paper, no ground reflection is included. The third octave spectrum is independent of tram running conditions and environment, and corresponds to full HVAC load. The reference third octave spectrum is measured at a standstill from the highest microphone of the directivity arc device. Empirical vertical directivity characteristics are encountered. The HVAC horizontal directivity is stated as uniform, which differs only slightly from the measurements.

3.2. Acoustic output variables and model validation

The empirical model delivers time-dependent quadratic acoustic quantities during the tram pass-by, either global A-weighted or in constant relative bandwidth bands (third octave bands). The time signature, corresponding to free-field sound pressure level at any fixed sensor position, is computed either for one, several or all source type(s) of the tram. Several standard acoustic event indicators are delivered, such as the maximum noise level L_{Amax} with Fast time constant, the equivalent sound pressure level $L_{Aeq,T}$ for the pass-by duration T, or the Sound Exposure Level.

The model has been validated in comparison with time signatures measured at different speeds on a microphone at standard position (distance 7.5 m, height 1.2 m), with all sources except HVAC. Fig. 16 provides the time signature contribution calculated for each source type ; peaks in the bogie signatures are associated with the pass-by of bogies, whose number differs from tram A to tram B. The validation microphone was placed along the tram line about 20 m away from the array position. In every case the two global time signatures agree very well with each other (Fig. 16 [4]). Discrepancies may occur in some third octave bands, mainly concerning the noise increase and decay that occur before and after the tram pass-by [19]. They probably result from mismatched directivities together with the omission of rail/track vibration decays on both sides of the

[4] On the site with stiff pads + grass, a local alteration of track surfacing prior to the microphone location induces an extra noise peak on the rising slope of measured signatures.

trams. This also agrees with the validation operated on time signatures provided by the highest directivity microphones (height 4.13 m), as illustrated by Figure 17 [3]. Although this point deserves further research, it does not imply meaningful effect on standard indicators since the measurement time is restricted to the pass-by time from head to end of the tram.

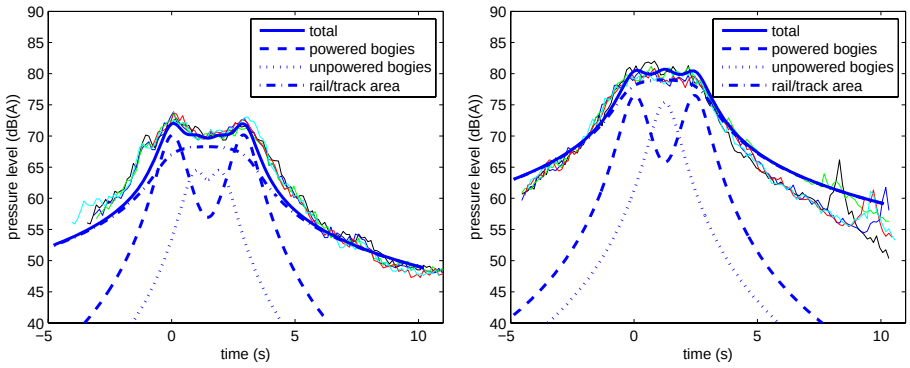

Figure 16: Global time signature at 7.5m, comparison model output for tram (thick solid line) / measurements (thin solid lines) — model output for each source type (thick broken lines) — speed 40 km/h — *left* : tram A on stiff pads + grass — *right* : tram B on soft pads + paving

A parallel may be drawn with the approach and model used in the European project SILENCE. In particular one of the tram is common to both studies (tram A, although with some version differences); however, distinct track types and choice of source areas make difficult the direct comparison with results available in [9]. Nevertheless, main source ranking and order of magnitude agree.

In the following, the tram noise emission model is used to assess the contribution of traction noise on one part and of HVAC on the other hand, to the emitted noise in free-field.

4. Contribution of traction noise

Among the source areas previously identified, powered bogies, unpowered bogies and the rail-track area all involve rolling noise. Powered bogies imply

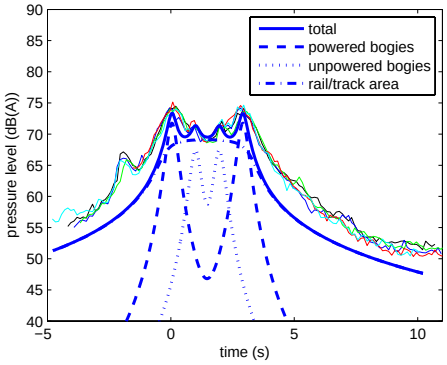

Figure 17: Global time signature at highest directivity microphone (distance 3.0 m, height 4.13 m), comparison model output for tram (thick solid line) / measurements (thin solid lines) — model output for each source type (thick broken lines) — speed 40 km/h — tram A on stiff pads + grass

the additional noise contribution from the neighbouring components associated with traction (motors and auxiliaries). As a first approximation, rolling noise originating respectively from powered and unpowered bogies can be assumed to be similar (thus inferring similar wheel roughnesses), since mass differences lead to effects of secondary importance. Then the relative part of rolling noise and traction noise may be assessed by using the previous free-field model and comparing the following cases, both without HVAC :

- rolling noise alone : every bogie area of the tram is granted with the characteristics of unpowered bogies, and the extended rail-track source is also included ;
- rolling noise + traction noise : the tram configurations comply with reality, that is they include powered bogies, unpowered bogies and the extended rail-track area.

The observer is located 7.5 m away from the track axis and 1.2 m high. In each case the standard global pass-by indicators have been calculated and compared. Figure 18 shows the L_{Amax}, with "rolling noise alone" and with

"rolling noise + traction noise", at several pass-by speeds and for the various tram/site combinations. Trends are similar for the maximum pressure level L_{Amax}, the equivalent noise pressure level L_{Aeq,T_p} or the exposure level, though heightened with the maximum level at pass-by, i.e. :

- on the "low noise" site : for tram A, of older generation, traction noise dependence on speed is higher than it is for rolling noise ; the opposite occurs for tram B, of more recent generation ;
- on the acoustically less favourable site : traction noise contribution for tram A is low, although with the same speed dependence as rolling noise ; it is insignificant for tram B.

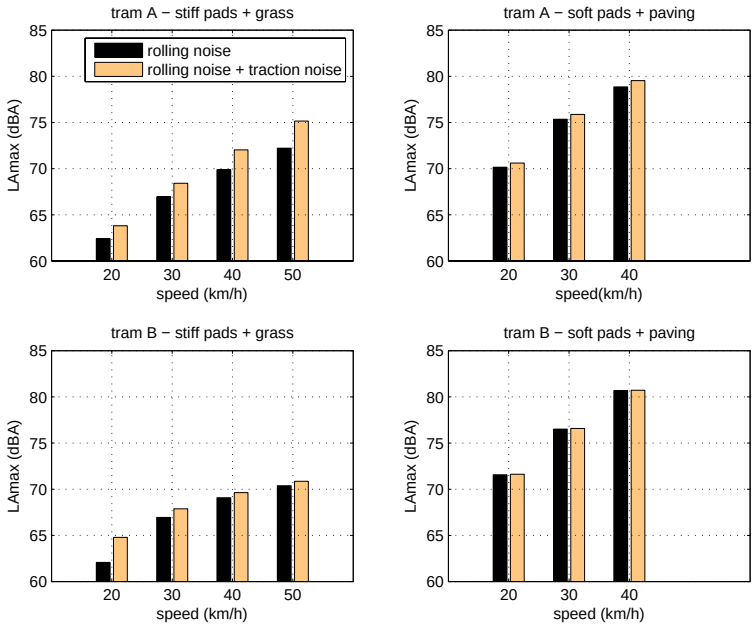

Figure 18: Maximum pressure level at 7.5m (height 1.2m) at a tram pass-by, either with rolling noise sources alone or with rolling noise + traction noise sources

This indicates that, for a site equipped with a track infrastructure favourable to low noise, tram emission modelling requires the inclusion of traction noise

sources in addition to the essential rolling noise sources, whereas in case of an acoustically unfavourable track, the traction contribution could be neglected when considering global noise indicators. However, this last conclusion becomes inappropriate when a spectral analysis should be carried out, since traction noise may contribute more strongly in some frequency bands, among other things through the presence of tones.

5. Contribution of HVAC

The noise source associated with HVAC differs from the other sources on several aspects : on one hand its location on the roof, on the other hand its operation which does not depend on the running conditions (speed) nor on the surroundings (type of track). The previous free-field tram emission model is used to analyse the HVAC contribution to the noise emitted by tram B [5], by comparing noise levels either with HVAC off or with full-working HVAC. The virtual measurement point is located 15 metres away from the track axis, and at several heights in order to study noise emission toward building storeys (from 2 metres up to 20 metres with 3 metre steps, ie. approximately each storey from ground floor to 6th floor). The 15 metre distance was selected here since it corresponds to the mean distance for all the residents questioned in the combined survey [1]. When the emission angle exceeds the valid angle range for the model, the vertical directivity is supposed to be constant above θ_{max}. Concerning the rolling noise sources, the emission angles remain within the validity range of the model. The cases of a low-noise track (stiff pads + grass) and of a noisier track (soft pads + paving) are studied.

The noise levels calculated at several heights depend largely on the respective powers and vertical directivities of the sources. As height rises, the received noise level increases at the very first storeys and then decreases on the "low noise" site, whereas it decreases continuously on the "noisier" site, whatever the speed

[5] Tram A has no HVAC equipment.

(Figure 19). Figure 20 shows the increase of the maximum A-weighted noise level when HVAC is working, relatively to the same situations without HVAC, for different observer heights: HVAC contribution is higher toward greater heights because of the lower part of the rolling noise sources offering a larger directivity toward lower heights. The relative HVAC noise part is obviously higher when rolling noise remains moderate, i.e. at low speed and/or on "low noise" sites where the increase may exceed 3.5 dB(A); on the "noisier" site, it is moderate at all speeds. These free-field observations remain available for streets with buildings on one side only, but should be reconsidered in case of canyon streets, taking account of the absorption properties of buildings and multiple reflections.

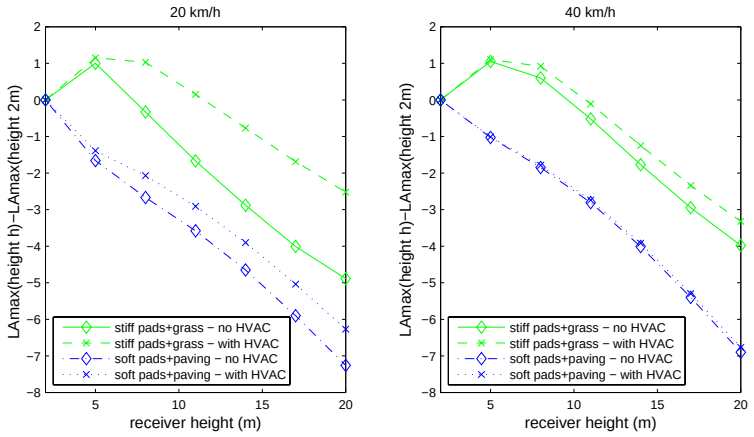

Figure 19: Increase of the free-field L_{Amax} with the receiver height without (resp. with) HVAC, at 20km/h and 40km/h – ref. level L_{Amax} at 2m height — distance to the track: 15m

6. Conclusions

An experimental study on tram noise emission has been conducted for two tramsets, representative of different French rolling stock generations, running at constant speed on two sites. Both sites differ by the track construction (mainly the pad stiffness) and the type of surfacing (grass or paving). The rail roughnesses could be measured only on a restricted wavelength range, the rails

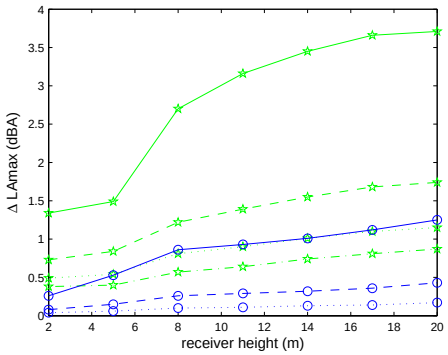

Figure 20: Difference of the free-field L_{Amax} with and without HVAC, as a function of the receiver height, distance to the track 15m; —⋆— stiff pads+grass 20km/h ; – –⋆– – stiff pads+grass 30km/h; · · ·⋆· · · stiff pads+grass 40km/h; · – ·⋆· – · stiff pads+grass 50km/h; —o— soft pads+paving 20km/h ; – –o– – soft pads+paving 30km/h; · · ·o· · · soft pads+paving 40km/h

were in good general state.

The analysis of the global noise power emitted for the whole tram indicated that the site with soft pads and a paved surface gives rise to +6 up to +10 dB(A) higher power levels than the one with stiff pads and a grass surface. Additional sound absorption measurements would be useful to distinguish the respective effects of track and surface types. The type of tram, even though influencing at a lower level, acts mainly on the spectrum and its modification with speed. The mean vertical directivity is similar for both trams but differs from one site to the other: approximately isotropic on the quieter site but more pronounced for low elevation angles on the noisier one. However directivities may differ in some third octave bands or near some noise source areas.

Noise source analysis at the tram pass-by were performed through a microphone array. Main sources are located near the ground; they concern the wheels and bogies, as well as an area which extends along the track from front to rear of the tram including the track radiation. Greatly led by rolling noise, they are much dependent on the track characteristics. Powered bogies include the extra contribution of traction noise (motors and neighbouring equipment),

resulting in additional frequency components dependent on speed and typical of each tram type. HVAC was the only source detected on the tram roof. It has been shown that HVAC may induce a sound pressure level increase exceeding 3 dB(A) towards building storeys when quiet rolling noise conditions are available. Therefore careful attention should also be applied by designers to noise emission of roof-mounted equipment.

The noise source identification method used in this research relies on classical microphone array processing. In the neighbourhood of the bogies, it does not allow the strict separation of the vehicle and track source contributions, which have been gathered within the radiation of the *bogie area*. The track noise source, occurring all along the tram and including the radiation of the vibrating rails, is mismatched with the usual source model underlying array processing. Further developments are necessary and are currently in progress to estimate railway track noise radiation more appropriately.

Finally, an empirical tram noise emission model, based on individual noise sources, has been developed. It forms a worthwhile tool for studying actual or virtual source contributions in various track and rolling stock configurations. The respective contributions of rolling and traction noise could thus be assessed. Further extension of the measurement database is now required to result in an operational inventory, diagnosis and analysis tool of trams in real world conditions and environment, as well as the connection with far-field propagation models.

Acknowledgements

This research was supported by the French Environment and Energy Management Agency (ADEME). The authors would also like to thank project partners SerdB and SEMITAN.

References

[1] Philipps-Bertin C., Champelovier P., Lambert J., Trindade C., Legouis T., Perception and annoyance due to tramway noise, Internoise 2007, Istanbul, Turkey, 2007.

[2] Maldonado M., Chiello O., Le Houedec D., Propagation of vibrations due to a tramway line. In: Springer Publications. Notes on Numerical Fluid Mechanics and Multidisciplinary Design (NNFM) - Noise and Vibration Mitigation, NNFM 99, pp. 158-164, 2008.

[3] Riemens S., New facts about noise emission of tramcars, Internoise 89, Newport Beach, USA, 1989.

[4] Spackova H., Noise reducing devices in the construction of tram permanent way in Prague, Internoise 2004, Prague, Tch. Rep., 2004.

[5] Lakusic S., Rukaniva T., Dragcevic V., The influence of the reconstruction of the tram tracks on the level of noise, Internoise 2005, Rio de Janeiro, Brasil, 2005.

[6] Piana E., Cousin G., Armani A., Beretta G.P., Characterization of ground vehicles noise emission by pass-by tests using an 8-microphone array, Internoise 2002, Dearborn, MI, USA, 2002.

[7] Dutilleux G., Tram noise - Source representation in prediction models. Workshop on noise reduction of road transportation, Aix-les-Bains, France, 2006 (in French).

[8] Pallas M. A., Lelong J., Investigation of the rolling noise sources on the tram of Nantes with a microphone array, Internoise 2001, The Hague, the Netherlands, 2001.

[9] Fillol C., Frid A., Poisson F., Report on source ranking on state of the art validation platforms and final priorities for research efforts, Deliverable E.D2, SILENCE Project, http://www.silence-ip.org .

[10] EN ISO 3095:2005, "Railway applications - Acoustics - Measurement of noise emitted by railbound vehicles", 2005.

[11] Johnson D. H., Dudgeon D. E., Array signal processing, Prentice Hall,1993.

[12] Brühl S., Schmitz K. P., Noise source localization on highspeed trains using different array types, Internoise 93, Leuven, Belgium, pp. 1311-1314, 1993.

[13] Elias G., Source localization with a two-dimensional focused array : optimal signal processing for a cross-shaped array, Internoise 95, Newport Beach, USA, pp. 1175-1178, 1995.

[14] Van Lier S., The vibro-acoustic modelling of slab track with embedded rails, Journal of Sound and Vibration 231(3), pp. 805-817, 2000.

[15] Pallas M. A., Perrier R., Nearfield noise source localisation with constant directivity arrays : a comparison - Application to tram noise, NAG/DAGA 2009, Rotterdam, the Netherlands, 2009.

[16] Pallas M. A., Lelong J., Chatagnon R., Tram noise emission : spectral analysis of the noise source contribution, Acoustics08, Paris, France, 2008.

[17] Kitagawa T., Thompson D. J., The horizontal directivity of noise radiated by a rail and implications for the use of microphone arrays, Journal of Sound and Vibration 329(2), pp. 202-220, 2010.

[18] Cato D. H., Prediction of environmental noise from fast electric trains, Journal of Sound and Vibration 46(4), pp. 483-500, 1976.

[19] Pallas M. A., Philipps-Bertin C., Maldonado M., et al., Noise and vibrations due to trams : emission and perception, INRETS, Les Collections de l'INRETS, 270 p., 2009 (in French).